Clin Exp Metastasis (2009) 26:955–964
DOI 10.1007/s10585-009-9286-3

RESEARCH PAPER

Osteoblasts modulate Ca^{2+} signaling in bone-metastatic prostate and breast cancer cells

Julia D'Ambrosio · Alessandro Fatatis

Received: 17 June 2009 / Accepted: 1 September 2009 / Published online: 21 September 2009
© Springer Science+Business Media B.V. 2009

Abstract Metastatic prostate and breast cancers display a predilection for the skeleton. The high incidence of skeletal metastasis may be a reflection of favorable reciprocal interactions between the bone microenvironment and disseminated cancer cells. Here we show that bone-metastatic PC3-ML prostate cancer cells and MDA-231 breast cancer cells—when co-cultured with human osteoblasts—down-regulate the increase in cytosolic free calcium (Ca^{2+}) induced by agonist stimulation. This osteoblast promoted alteration of Ca^{2+} signaling develops and reverts in a time-dependent manner. Most importantly, the Ca^{2+} responses of cancer cells lacking bone metastatic potential are not affected by osteoblasts. The limited increase in cytosolic Ca^{2+} observed in bone-metastatic cells does not result from depleted intracellular Ca^{2+} stores but rather a decreased entry of Ca^{2+} from the extracellular space. Interestingly, the inhibition of histone deacetylase in cancer cells replicates the changes in Ca^{2+} signaling induced by osteoblasts, suggesting the participation of epigenetic mechanisms. Finally, cancer cells harvested from skeletal metastases induced in mice showed Ca^{2+} responses identical to cells co-cultured with osteoblasts. However, Ca^{2+} signaling in cancer cells recovered from metastases to soft-tissues was not affected, emphasizing the role of the bone microenvironment in regulating the functional behavior of bone-metastatic cells. We propose that osteoblasts protect selected malignant phenotypes from cell death caused by an excessive increase in cytosolic Ca^{2+}, thereby facilitating their progression into macroscopic skeletal metastases.

Keywords Metastasis · Bone microenvironment · Osteoblast · Calcium signaling

Introduction

The ability of disseminated cancer cells to survive in the bone marrow and eventually progress into clinically relevant metastases relies on their inherent capability of establishing symbiotic interactions with resident cells of the bone microenvironment [1, 2]. In general, both normal and malignant cells maintain low levels of cytosolic free Ca^{2+} ($[Ca^{2+}]_c$) while allowing moderate and temporary increases of this second messenger in response to extracellular signals [3]. A fine-tuning of this process is essential to cellular homeostasis, as its deregulation almost invariably leads to toxic insults and can ultimately trigger cell death by either necrosis or apoptosis [4, 5]. This paradigm would especially apply to cancer cells disseminated to the skeleton, as matrix degradation—during either physiological bone remodeling or pathological osteolysis—releases large amounts of Ca^{2+} into the local milieu [6]. The extensive and prolonged stimulation of these cancer cells by growth factors, cytokines and hormones present in the bone marrow, combined with the constant availability of elevated extracellular Ca^{2+}, could negatively affect long-term cellular survival [7–9].

Electronic supplementary material The online version of this article (doi:10.1007/s10585-009-9286-3) contains supplementary material, which is available to authorized users.

J. D'Ambrosio · A. Fatatis (✉)
Department of Pharmacology and Physiology, Drexel University College of Medicine, 245 N. 15th Street, New College Building, MS488 Philadelphia, PA 19102, USA
e-mail: afatatis@drexelmed.edu

A. Fatatis
Department of Pathology and Laboratory Medicine, Drexel University College of Medicine, Philadelphia, PA 19102, USA

The present study shows that prostate and breast cancer cells lacking bone-metastatic potential display uniform Ca^{2+} responses when exposed to different agonists. In contrast, bone-metastatic cells respond in a heterogeneous fashion, either activating or down-regulating Ca^{2+}-entry pathways. We also found that normal human osteoblasts accentuate these constitutive features of bone-metastatic cancer cells, by promoting the down-regulation of Ca^{2+} influx through the production of one or more soluble factors.

The control of Ca^{2+} homeostasis is directly linked to cell survival, as excessive $[Ca^{2+}]_c$ can either directly activate the apoptotic cascade or induce necrotic death [3–5]. Interestingly, most disseminated cancer cells die in secondary organs rather than colonize the tissue and progress into macroscopic metastases [10]. For instance, we have recently reported that of three different human prostate cancer cell lines, PC3-ML cells progress into macroscopic metastases, whereas DU-145 and PC3-N cells do not survive past the first week following their arrival to the skeleton [11].

Thus, cancer cells that successfully adapt to the bone microenvironment by limiting the influx of Ca^{2+} and its excessive cytosolic increase might resist cell death, and ultimately produce macroscopic metastases. In contrast, cells lacking these capabilities may arrive to the skeleton only to eventually succumb to the exceedingly large amounts of Ca^{2+} that are locally available.

Results and discussion

In the initial part of this study we aimed to establish whether cancer cells with different bone-metastatic behaviors in animals also differed in their Ca^{2+} signaling properties. To this end, human prostate and breast cancer cells were stimulated with agonists of plasma-membrane G-protein-coupled receptors (GPCRs) and their Ca^{2+} responses evaluated. We used adenosine triphosphate (ATP), which elicits Ca^{2+} signals in a variety of normal and malignant cells through the stimulation of P2 purinergic receptors [12, 13]. This agonist was also selected because of its important role in maintaining skeletal architecture, exerted by stimulating the proliferation of bone marrow stromal cells (BSCs) in a paracrine fashion [14]. Thus, a first set of experiments was conducted with the prostate cancer cell lines DU-145 and PC3-N and breast cancer cell line MDA-468. These cell lines fail to produce macroscopic skeletal metastases in experimental animals, as others and we have previously established [11, 15–17]. When individual cells for each cancer cell line were examined, we found that ATP uniformly induced a rapid increase of $[Ca^{2+}]_c$ followed by a minor decrease and a prolonged plateau, which lasted until the removal of the agonist from the extracellular milieu (Fig. 1a). In contrast, when bone-metastatic PC3-ML prostate cancer cells [11] and MDA-231 breast cancer cells [18] were exposed to ATP, a heterogeneous spectrum of Ca^{2+} responses was observed (Fig. 1b). For instance, $65 \pm 7\%$ of PC3-ML cells and $82 \pm 5\%$ of MDA-231 cells generated Ca^{2+} responses identical to non-bone metastatic cells. This group included cells in which the Ca^{2+} plateau measured in magnitude at least 70% of the $[Ca^{2+}]_c$ values reached by the preceding peak. These cells were conventionally named *High-Plateau* (HP). A second group of cells was identified by Ca^{2+} responses showing a plateau with a magnitude equivalent to 30% or less than the $[Ca^{2+}]_c$ values reached by the preceding peak. This second type of response was observed in $7 \pm 3\%$ of PC3-ML cells and $6 \pm 2\%$ of MDA-231 cells, which were named *Low-Plateau* (LP). Finally, a third group of cells showed responses with a Ca^{2+} plateau of a magnitude comprised between 30 and 70% of the $[Ca^{2+}]_c$ values reached by the preceding peak (Fig. 1b–d). When PC3-ML and MDA-231 cells were exposed to carbachol (CCh)—which stimulates muscarinic GPCRs—this agonist generated Ca^{2+} responses that mimicked those induced by a previous exposure of the same cells to ATP (**S1**). This suggests that the multiple types of Ca^{2+} responses observed in bone-metastatic cells occur consistently and independently of the type of GPCR stimulated. Because of the extremely fertile environment for cellular trophism and proliferation provided by the bone marrow and the central role of Ca^{2+} signaling in regulating these phenomena, it seems likely that, in addition to ATP, this peculiar responsiveness of bone-metastatic cells may affect the activity of several other growth and survival factors. However, a similar scenario could be also observed if the PC3-ML and MDA-231 cell lines were harboring multiple sub-populations, each generating a distinct Ca^{2+} response. This possibility was investigated by treating cells with three consecutive pulses of ATP over a 24 h time interval and recording the agonist-generated Ca^{2+} responses. Interestingly, we found that in both PC3-ML and MDA-231 populations, individual cells could over time spontaneously switch from HP to LP Ca^{2+} responses and vice versa (**S2**). In addition, cells generating a Ca^{2+} response with a plateau of intermediate magnitude were most likely transitioning between HP and LP-responsive states as shown in Fig. 1b. Overall, the intrinsic mechanism responsible for this phenomenon seems to favor HP responses, as suggested by the lower percentage of LP-responding cells detected at any given time.

A widely accepted paradigm is that symbiotic interactions established between the tissue microenvironment and disseminated cancer cells may underlie the metastatic organ tropism that characterizes most tumors [1], and in particular the propensity of prostate and breast cancers to

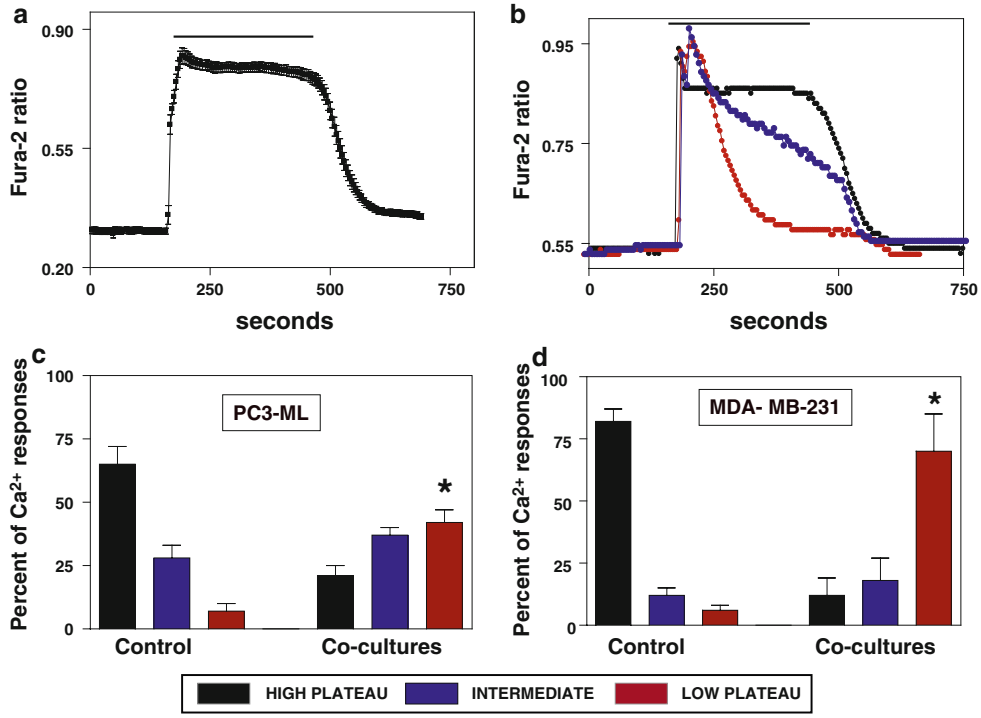

Fig. 1 Agonist-induced Ca^{2+} responses observed in prostate and breast cancer cells with different bone-metastatic potential. **a** Non bone-metastatic PC3-N and DU-145 prostate cancer cells and MDA-468 breast cancer cells were exposed to 100 μM ATP for 5 min (*black horizontal line*) and showed a rapid peak of increase in cytosolic free Ca^{2+} followed by a sustained and prolonged plateau in all cells examined; **b** In contrast, ATP induced three different types of Ca^{2+} responses in bone-metastatic PC3-ML prostate cancer cells and MDA-231 breast cancer cells. A first response was similar to that observed in non bone-metastatic cells and defined by a Ca^{2+} plateau measuring 70% or more of the initial peak's magnitude. This response was named *High Plateau* (*black trace*). A second type of response was characterized by a much lower Ca^{2+} plateau, which represented only 30% or less of the initial peak's magnitude. This response was named *Low Plateau* (*red trace*). Finally, Ca^{2+} responses displaying plateau values comprised between 70 and 30% of the initial peak's magnitude were named *intermediate* and included in a third group (*blue trace*). The magnitude of the Ca^{2+} plateau for each individual cell was arbitrarily measured at 2.5 min after the onset of the response to ATP. There were no significant differences in the extent of the initial Ca^{2+} peak between the bone-metastatic and non bone-metastatic cells. *Traces* are from representative individual cells. The relative percentage of High Plateau (HP) responses (*black columns*) was considerably higher than Low Plateau (LP) responses (*red columns*) both in PC3-ML (**c** control) and MDA-231 cells (**d** control). Cells displaying a Ca^{2+} plateau of intermediate magnitude between that of HP and LP responding cells represented 28 ± 4 and 12 ± 3% of PC3-ML and MDA-231 cells, respectively (*blue columns*). The total number of cells analyzed for each cell line were as follows: DU-145: 167 cells in five experiments; PC3-N: 150 cells in three experiments; MDA-468: 158 cells in nine experiments; PC3-ML: 279 cells in eight experiments; MDA-231: 376 cells in eight experiments. The relative percentage of LP responses in both PC3-ML and MDA-231 cells was dramatically increased by 7 day co-culture with human osteoblasts (**c**, **d**). The total number of cells analyzed for these sets of experiments were as follows: PC3-ML: 600 cells in 19 experiments; MDA-231: 148 cells in five experiments (*$P = 0.0004$ for PC3-ML; * $P = 0.0002$ for MDA-231). Co-cultures in which the same type of cancer cells investigated replaced the osteoblasts showed no changes in frequency or kinetic of agonist-induced Ca^{2+} responses

target the skeleton [2]. Thus, in the next experiments we explored the possibility that cells of the bone marrow stroma could promote further the intrinsic Ca^{2+} signaling properties of PC3-ML and MDA-231 cells.

To this end, we established co-cultures of either prostate or breast cancer cells with normal human osteoblasts obtained from male or female donors, respectively. After 7 day co-cultures, both PC3-ML and MDA-231 cells showed a dramatic change in their relative distribution of Ca^{2+} responses generated by ATP stimulation (Fig. 1c, d). For instance, the presence of osteoblasts increased the percentage of LP-responsive PC3-ML cells from 7 ± 3 to 42 ± 5%, with an almost comparable decrease in HP responses. This effect was even more noticeable in MDA-231 cells, in which the co-culture with osteoblasts induced an increase in LP responses from 6 ± 2 to 70 ± 15% (Fig. 1d). In contrast, non bone-metastatic cells—i.e., PC3-N and DU-145 prostate cancer cells or MDA-468 breast cancer cells—were not affected in their Ca^{2+} responses to GPCR agonists when co-cultured with osteoblasts (Supplemented Table 1).

Following their dissemination to the skeleton, cancer epithelial cells can be found in close proximity to hematopoietic tissue as well as metabolically active supporting stroma [19]. Indeed, stromal cells may replicate the effects exerted by osteoblasts on bone-metastatic cells, through

soluble mediators and/or cell–cell contact interactions. To investigate this possibility, PC3-ML cells were co-cultured with either bone Mesenchymal (MSCs) [20, 21] or Stromal (BSCs) [22, 23] cells obtained from human donors. We found that BSCs were ineffective in altering Ca^{2+} signaling in PC3-ML cells, whereas MSCs showed only a limited effect, decreasing the HP responses while leaving LP responses unaltered. In contrast, immortalized human Fetal Osteoblasts (hFOB) significantly changed the relative percentages of both HP and LP Ca^{2+} responses, similarly to what was previously shown by normal osteoblasts (**S3**). Taken together, these results indicate that the bone microenvironment could indeed alter Ca^{2+} signaling in disseminated cancer cells. However, this phenomenon seems to be restricted only to cells that are selectively equipped to respond to the effects exerted by osteoblasts.

Previous studies by others have reported changes in either cell viability or cell-cycle progression of human cancer cells co-cultured with immortalized murine osteoblasts [24]. The possibility that similar events could underlie the alterations in Ca^{2+} signaling in PC3-ML and MDA-231 that we observed was addressed by the next experiments. Bone-metastatic cancer cells co-cultured with osteoblasts were exposed to an antibody directed against the cleaved form of caspase-3, a mediator of apoptotic cell death [25]. When tested by immunofluorescence, these cells showed a negligible percentage of positive staining for the active caspase. Furthermore, the effect exerted by osteoblasts on the progression of cancer cells through the cell cycle was investigated by FACS analysis. PC3-ML and MDA-231 cells both showed a relative distribution of different cell cycle phases identical to cells cultured in the absence of osteoblasts (Fig. 2a, b) and significantly different from that of cells induced into quiescence by serum deprivation (Fig. 2c). Finally, co-cultured cancer cells were analyzed for their Ca^{2+} responses and subsequently tested for Ki-67, a nuclear protein expressed by cycling cells but absent in quiescent cells [26]. We found that Ca^{2+} signaling in bone-metastatic cells is unrelated to KI-67 expression, as HP and LP Ca^{2+} responses were observed with comparable frequency in cycling and quiescent cancer cells (Fig. 2d–f). Thus, these results indicate that the changes in Ca^{2+} signaling induced in PC3-ML and MDA-231 cells by human osteoblasts are determined by mechanisms different from either pro-apoptotic stimuli or alteration in cell cycle progression.

When osteoblasts are removed from the co-culture, bone-metastatic cancer cells revert to their original Ca^{2+} signaling properties within 48 h; this interval is shortened to just 9 h by the additional replacement of the osteoblasts-conditioned medium (**S4**). This rapid phenomenon could be the result of genomic plasticity, which may occur through epigenetic regulation. Indeed, recent studies emphasize the role of epigenetic mechanisms in the interactions between stromal microenvironment and tumor cells [27, 28]. Modulation of gene expression can be obtained by regulating the accessibility of DNA to the transcription machinery. This is achieved through DNA methylation and/or chromatin alterations induced by histone modifications [29, 30]. To investigate this possibility, we used pharmacological compounds capable of affecting the epigenetic machinery in bone-metastatic cancer cells cultured alone, in the attempt to reproduce the changes in Ca^{2+} signaling induced by the presence of osteoblasts. An inhibitor of DNA methylation, 5-Aza-2′-deoxycitidine (2.5 μM for 24 h) [31] was ineffective in altering the Ca^{2+} signaling properties of PC3-ML and MDA-231. However, the inhibitor of histone-deacetylase trichostatin-A (100 nM for 24 h) [32] increased acetylated histone-H3 in PC3-ML cells to 282% above control levels and significantly altered the relative distribution of HP and LP Ca^{2+} responses in bone-metastatic cells (**S5**). These observations were corroborated by the increase in acetylated histone-H3 detected in PC3-ML cells co-cultured with osteoblasts (208% above control levels). The removal of trichostatin A from cultures of PC3-ML and MDA-231 cells restored the normal percentages of HP and LP Ca^{2+} responses within 24 h (**S5**), similarly to what was observed upon withdrawal of the osteoblasts-conditioned medium from co-cultured bone-metastatic cells (**S4**). Thus, one or more soluble factors secreted by osteoblasts appear to modulate Ca^{2+} signaling exclusively in bone-metastatic cancer cells, in a reversible fashion and through the intervention of the histone-deacetylase. Reduction in magnitude and/or duration of Ca^{2+} signals has been previously described in different cell types and attributed to rapid receptor desensitization [33, 34]. However, PC3-ML and MDA-231 cells consistently responded with either HP or LP kinetics when consecutively exposed to ATP (Fig. 3a), thus ruling out receptor desensitization as a possible cause for the reduced Ca^{2+} plateau phase characterizing the LP response. On the other hand, the removal of extracellular Ca^{2+} completely abolished the differences between LP and HP responding cancer cells, indicating that an increased Ca^{2+} influx is the most plausible explanation for the larger Ca^{2+} plateau phase observed during HP responses (Fig. 3b). The lack of extracellular Ca^{2+} eliminated also the small plateau in LP-responsive cells, indicating that also at this stage bone-metastatic cells allow some Ca^{2+} entry, albeit of a much lower magnitude than HP-responding cells. It should be emphasized that an influx of extracellular Ca^{2+} can occur with minimal or even undetectable increase in $[Ca^{2+}]_c$, as reported for endothelial or astroglial cells among others [35, 36]. This mechanism ensures the proper refilling of the intracellular calcium stores (ICS) and, as shown in LP responsive cells, is effective in preserving Ca^{2+} signaling

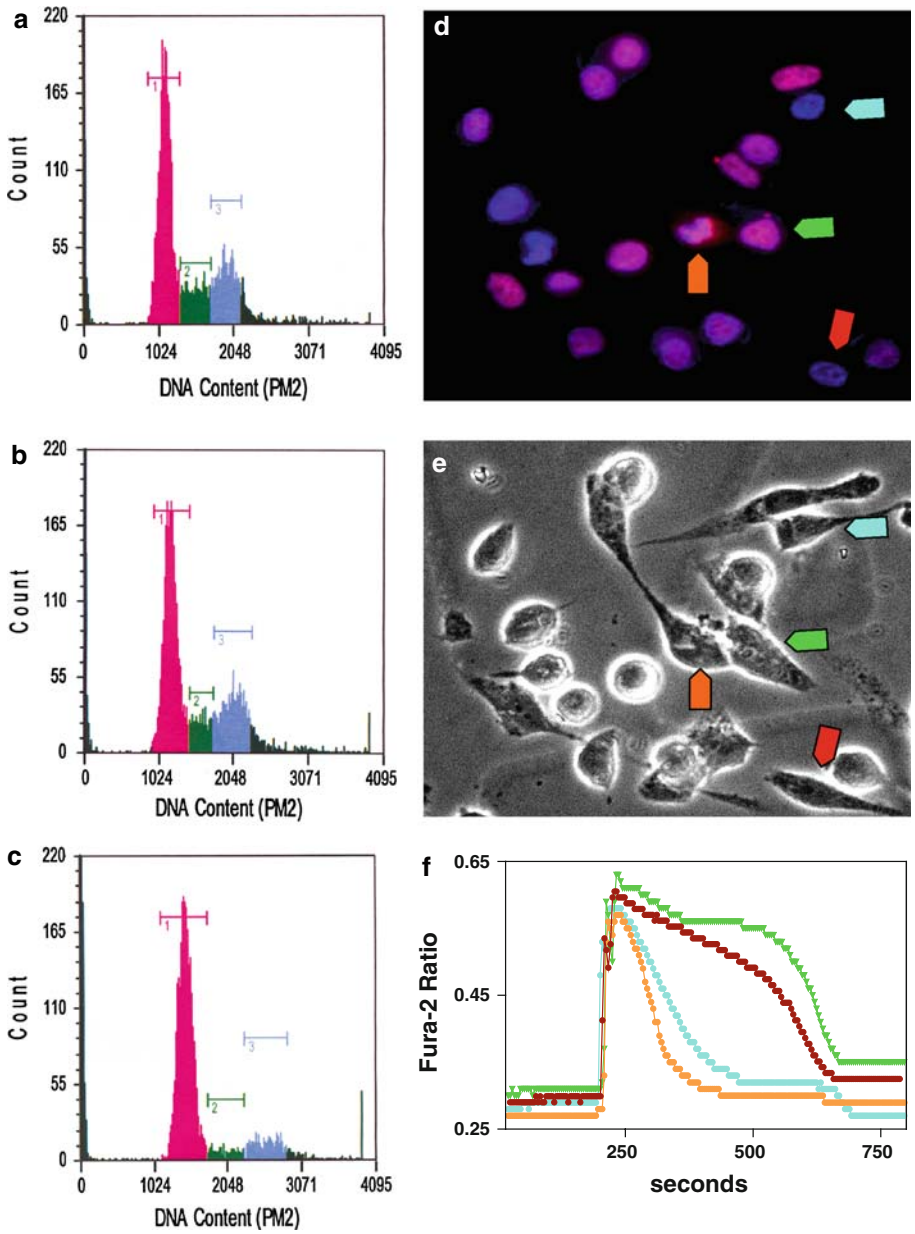

Fig. 2 Analysis of cell cycle phase distribution and Ki-67 expression in bone metastatic cancer cells co-cultured with osteoblasts. Bone-metastatic PC3-ML prostate cancer cells and MDA-231 breast cancer cells were cultured in the absence or presence of normal human osteoblasts for 7 days and analyzed by FACS. Co-cultured cells displayed a normal cell cycle phase distribution (**a**) and were identical to untreated and asynchronous cells (**b**). Cells deprived of serum for 72 h displayed an increase in the accumulation of cells in G0/G1 phase with subsequent decreases in G2/M and S phases, as expected [50] (**c**). The data shown are from one of four representative experiments (2 each for PC3-ML and MDA-231 cells). G0/G1 phase = *red peak*; S phase = *green peak*; G2/M phase = *blue peak*. To establish whether HP and LP Ca^{2+} responses to ATP were correlated to changes in Ki-67 expression, cells were plated on photo-etched glass coverslips. At the end of each experiment, the imaged cells were identified using photo-etching guidance, labeled with an anti-Ki-67 antibody (*red signal*) and DAPI nuclear staining (*blue signal*) and examined by fluorescence microscopy (**d**, **e**). Quiescent cells show only *blue* nuclear staining, whereas proliferating cells display a *pink* staining deriving from the overlay of DAPI and Ki-67 fluorescent signals. HP and LP Ca^{2+} responses were unrelated to Ki-67 staining and occurred with comparable frequency in proliferating and quiescent cancer cells (**d**, **f**). Quiescent cells = *blue* and *red arrows* (**d**, **e**) and calcium signaling traces (**f**); proliferating cells = *green* and *orange arrows* (**d**, **e**) and calcium signaling traces (**f**)

upon sequential agonist stimulations (Fig. 3a). These observations lead us to hypothesize that, although the larger Ca^{2+} influx in HP-responsive cells seems not to be required for complete ICS filling and proper functioning, it could potentially increase cell vulnerability to deregulation of Ca^{2+} homeostasis and subsequent death [37].

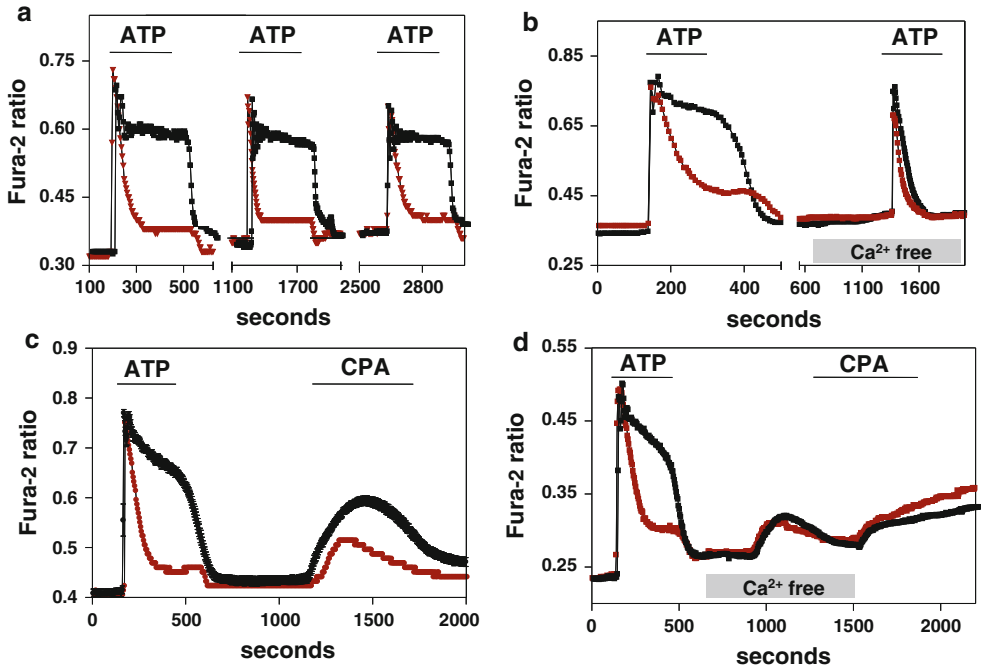

Fig. 3 Analysis of the Ca^{2+} signaling events characterizing the High Plateau and Low Plateau responses observed in prostate and breast cancer cells. PC3-ML cells were repeatedly exposed to ATP (10 μM for 5 min), with 10 min intervals separating agonist stimulations in which ATP was washed out from the perfusion chamber. Each single cell analyzed consistently produced a response with the same HP or LP kinetic upon each individual ATP pulse. Similar results were obtained using the muscarinic agonist CCh (10 μM). Traces are from two representative cells (**a**); the removal of extracellular Ca^{2+} abolished the high plateau observed in HP responsive PC3-ML cells as well as the plateau of much lower magnitude characterizing the LP responses (**b**); PC3-ML cells previously identified as HP or LP-responsive to ATP stimulation were subsequently exposed to 10 μM CPA (**c**). This reversible inhibitor of the SERCA pump induced an increase in cytosolic Ca^{2+} of significantly higher magnitude in HP-responsive cells as compared to cells producing LP responses and established by calculating the area *under the curve* (HP 62 ± 10 vs. LP 27 ± 5, arbitrary units). In contrast, cells exposed to CPA in the absence of extracellular Ca^{2+} mobilized the ICS to the same extent (HP 12 ± 2 vs. LP 11 ± 1, arbitrary units) (**d**). Upon re-addition of extracellular Ca^{2+}, a sustained increase in $[Ca^{2+}]_i$ was observed in all cells analyzed, regardless of the type of response previously induced by ATP (**d**). Calcium free conditions were obtained by adding 100 μM EGTA to virtually Ca^{2+} free solutions. Traces represent the average of all HP and LP responses recorded in a typical experiment. At least two separate experiments were conducted for each condition

The Ca^{2+} entry pathways operating in cancer cells during HP and LP responses were investigated using cyclopiazonic acid (CPA), a reversible inhibitor of the ER Ca-ATPase (SERCA) [38]. The SERCA continuously pumps Ca^{2+} from the cytosol back into the ER to counterbalance the constitutive slow egress of Ca^{2+} from ICS, thereby maintaining intracellular ICS replenished. Because of its functioning, the inhibition of SERCA progressively depletes ICS and consequently increases $[Ca^{2+}]_c$ [39]. A widely reported consequence of Ca^{2+} mobilization from ICS is the opening of store-operated channels in the plasma membrane, to allow the influx of extracellular Ca^{2+} and the refilling of ICS [40, 41].

When cells generating LP responses to ATP were successively exposed to CPA, $[Ca^{2+}]_c$ increased because of both ICS release and store-operated Ca^{2+} influx. The latter was clearly lower in magnitude as compared to HP-responding cells studied in identical conditions (Fig. 3c), thus confirming what was previously observed upon GPCR stimulation. This observation suggests that the Ca^{2+} signaling properties of PC3-ML and MDA-231 cells are unrelated to the type of stimulated cell-surface receptors and rather reflect singular differences in their Ca^{2+} signaling machinery, as compared to non bone-metastatic cells. However, when CPA was administered in the absence of extracellular Ca^{2+} (Fig. 3d), the ICS were depleted but the store-operated Ca^{2+} influx could not occur. In these conditions, the degree of Ca^{2+} released from ICS was comparable between HP and LP responsive cells. This indicates that the extent of ICS refilling following GPCR stimulation of bone-metastatic cells is not affected by the magnitude of Ca^{2+} entry. Upon the subsequent re-addition of extracellular Ca^{2+}, the store-operated influx was similar in HP and LP responsive cells. A possible explanation for this crucial observation is that the larger Ca^{2+} influx observed in HP cells is promoted by elevated $[Ca^{2+}]_c$, such as that produced by SERCA blockade or GPCR stimulation. For instance, if ICS are first depleted in Ca^{2+}-deprived extracellular medium and the extracellular Ca^{2+} is restored only when $[Ca^{2+}]_c$ had

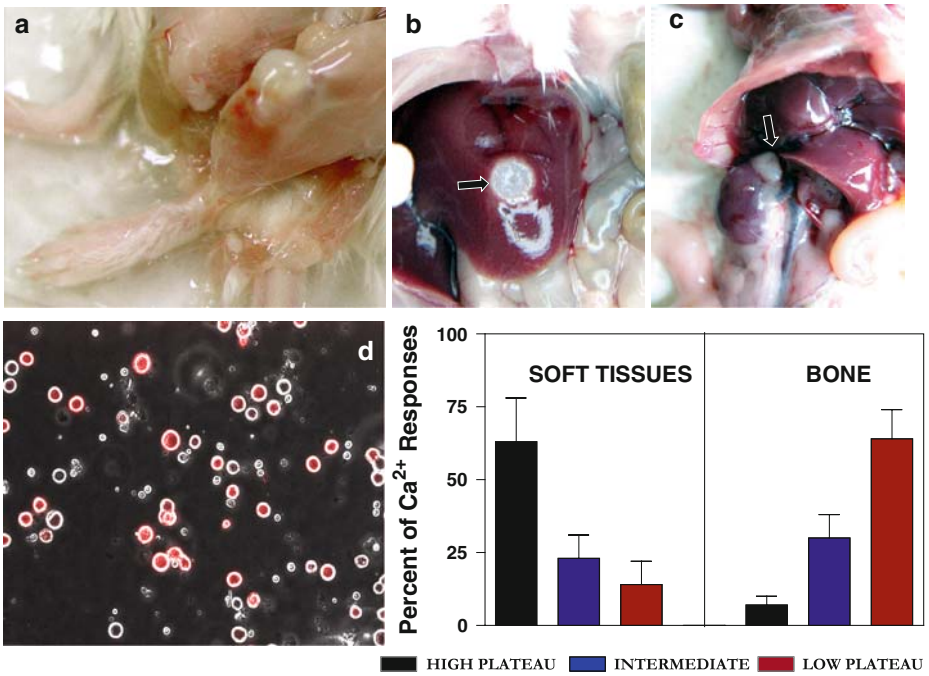

Fig. 4 Agonist-induced Ca^{2+} signaling in cancer cells collected from experimental metastases at the skeleton or in soft-tissue organs. PC3-ML prostate cancer cells inoculated in SCID mice via an intra-cardiac route produce metastatic tumors in the hind-leg that become macroscopically visible after 4 weeks (**a**). Upon necroscopy examination of internal organs, small tumors were also frequently observed in the adrenal glands and rarely in the liver (**b**, **c**). Cancer cells from experimental metastases—acutely dissociated in culture—were distinguished from normal murine cells by their red fluorescence deriving from stable expression of the DsRed2 protein (**d**). PC3-ML cells derived from skeletal tumors display an increase in LP responses to ATP—and a corresponding decrease in HP responses—similar to that observed in the same cells co-cultured with human osteoblasts. In contrast, agonist-induced Ca^{2+} signaling in cells derived from soft-tissue tumors was unaffected (**e**). These experiments analyzed 168 cancer cells collected from the skeleton and 35 cells from soft-tissues (adrenal gland and liver combined) (* $P < 0.0001$)

returned to pre-stimulation values, the additional Ca^{2+} influx responsible for generating HP responses is not recruited (Fig. 3d).

The identification of the plasma membrane Ca^{2+} channels responsible for generating the HP responses could lead to novel approaches aiming to irreversibly alter Ca^{2+} homeostasis in bone-metastatic cells and ultimately counteract their progression at the skeletal level.

Because of the translational implications of our study, an aspect of paramount importance was to validate the in vitro observations in an animal model. To this end, we inoculated PC3-ML prostate cancer cells in the left cardiac ventricle of SCID mice, a procedure that consistently produces metastases in femur and tibia of $\geq$80% animals, as we previously reported [11, 42] (Fig. 4a). Despite their strong bone-seeking phenotype, PC3-ML cells can also target soft tissues such as liver and adrenal glands, although these organs never develop large metastases (Fig. 4b, c). Thus, PC3-ML cells-engineered to stably express the DsRed2 fluorescent protein—were inoculated in mice and after 4 weeks recovered from metastatic tumors in the leg, liver and adrenal glands. After being acutely dissociated and plated on glass coverslips, cancer cells were distinguished from the murine host cells based on their red-spectrum emitted fluorescence (Fig. 4d). Imaging experiments conducted within 3 h from harvesting showed that cells deriving from bone metastases and exposed to ATP produced predominantly LP Ca^{2+} responses, confirming the results obtained in vitro with the osteoblast co-cultures (Fig. 4e). Remarkably, PC3-ML cells collected from metastases in soft-tissues and exposed to ATP showed a percentage of HP and LP Ca^{2+} responses similar to that observed in cells cultured alone (Fig. 4e).

In conclusion, cancer cells obtained from skeletal metastases and with demonstrated bone-tropism in animal models can constitutively down-regulate their Ca^{2+} influx in response to GPCR stimulation. This intrinsic feature is dramatically emphasized by osteoblasts, which through the apparent secretion of one or more soluble factors promote Ca^{2+} responses characterized by a very limited Ca^{2+} plateau.

Skeletal metastases have been routinely divided in osteolytic and osteoblastic (osteosclerotic) and different bone-metastatic tumors associated with either one type or the other. According to this paradigm, prostate cancer would induce predominantly osteoblastic bone lesions,

whereas lesions from breast cancer would be mostly osteolytic. However, this concept is currently being progressively replaced by the view that areas of osteosclerosis and osteolysis are very frequently coexisting in the same bone metastatic lesions from both breast and prostate cancers. In addition, in order for tumor cells to grow, invade mineralized bone and produce sclerotic tissue, osteolysis must first occur. Because of the high content of calcium deposited in the bone matrix, its degradation will release ionized calcium in the bone marrow microenvironment. An excessive increase in $[Ca^{2+}]_c$ almost invariably leads to impairment of mitochondrial functioning and activation of a series of events causing cell death [43]. This paradigm has been found to be particularly significant in cancer cells, in which increased influx of extracellular Ca^{2+}—separately or in combination with excessive depletion of intracellular Ca^{2+} stores—dramatically and negatively affect proliferation and survival [44–46].

Therefore, the mechanism we describe here could endow selected malignant phenotypes with a particular propensity for surviving in the bone microenvironment and successfully progress into clinically relevant metastases. The identification of the structural and regulatory molecules involved in this process could provide potential therapeutic targets for counteracting the growth of cancer cells disseminated to the skeleton.

Materials and methods

Cell lines and cultures

All cancer cell lines were purchased from American Type Culture Collection (Manassas, VA) and cultured in DMEM Mediatech, Inc., (Herndon, VA) plus 10% fetal bovine serum (Hyclone, Logan, UT) and 0.1% gentamicin (Invitrogen Corporation, Carlsbad, CA). PC3-N and PC3-ML human prostate cancer sub-lines, derived from the widely used PC3 parental line, were previously selected based on their different invasiveness in vitro and metastatic potential in animal models [47]. hFOB 1.19 human fetal osteoblasts (ATCC) were cultured at 34°C and 5% CO_2 in DMEM/F12 (Invitrogen) supplemented with 10% fetal bovine serum and Geneticin (400 ug/mL). Normal human osteoblasts (NHOs) from male and female donors (Lonza Biosciences, Walkersville, MD) were grown in osteoblast basal medium supplemented with bullet kit (Lonza). Human bone marrow stromal cells (HBSCs) and human bone mesenchymal stem cells (HMSCs) were grown as indicated by the commercial source (Lonza). For co-cultures, cancer cells were seeded at a density of 2×10^4 cells onto 15 mm glass coverslips placed in 60-mm culture dishes containing small paraffin footing (Paraplast, Kendall, Mansfield, MA). Thermanox plastic discs (Grace Bio-labs, Bend, OR) were used to support the human bone cells and prepared by drilling small holes spaced 0.5–1 cm apart throughout the surface to allow an effective exchange of gases and solutes throughout the culture dish. The discs received bone cells at a 1×10^6 final density. At the start of co-cultures, Thermanox discs with bone cells were placed downwards, facing the cancer cells and resting on the paraplast footing, as we previously described for different studies [48]. The type of bone cells in each co-culture dictated the growth medium used. A first set of control experiments ascertained that there were no changes in Ca^{2+} signaling for each type of cancer cell when cultured alone in the same media used for the co-cultures.

In addition, we established co-cultures in which the Thermanox discs supported the same type of cancer cells investigated rather than osteoblasts. Imaging experiments in these conditions failed to show any of the alterations of Ca^{2+} responses we observed in co-cultures including human osteoblasts. This observation seems to exclude that physical alterations of the in vitro culture microenvironment caused by the close vicinity of the two cellular monolayers—such as for example hypoxic conditions—are primarily responsible for the modulation of Ca^{2+} signaling in bone-metastatic cancer cells that we report in the present study.

Reagents and chemicals

ATP, EGTA, CCh and Trichostatin-A were purchased from Sigma (St. Louis, MO). TG and CPA were purchased from Calbiochem (San Diego, CA). Fura-2/AM was purchased from Invitrogen (Molecular Probes, Eugene, OR).

Single-cell intracellular calcium measurements

Cells growing on glass coverslips were loaded with 2 μM Fura-2/AM for 20 min in a balanced salt solution, as previously described [49]. Coverslips were mounted on a RC-25F laminar flow perfusion chamber (Warner Instrument Corporation, Hamden CT) and placed on the stage of an IX70 inverted microscope (Olympus, Center Valley PA). Experimental solutions were perfused using a micro pump (Instech Lab Inc., Plymouth Meeting, PA) with a flow rate set at 650 μL per min. Temperature throughout the experiment was maintained between 26 and 29°C using a TC-324B heater controller (Warner). A two-way valve (Thomson, Springfield VA) regulated the flow of agonist-containing solutions from an injection loop to the perfusion chamber. The removal of the experimental solutions from the chamber was achieved using a suction tube connected to a peristaltic pump (Gilson Inc., Middleton, WI). A lambda DG4 Xenon UV-light source (Sutter, Novato CA)

controlled by computer was used to alternate excitation wavelengths at 340 and 380 nm. Emitted fluorescence was acquired at 520 nm wavelength and images were collected every 5 s using a 20× objective and a charge-coupled device (CCD) intensified MicroMax 1300YHS camera (Roper Scientific, Trenton, NJ). Fura-2 emitted fluorescence from each cell in the imaged population was acquired and analyzed independently using the Metafluor software (Molecular Devices, Downingtown, PA). For experiments performed under Ca^{2+} free conditions, medium was prepared omitting $CaCl_2$ and adding 100 μM EGTA.

Animal model of experimental metastasis

The mouse model of experimental metastasis used was developed in our laboratory [10, 14]. Briefly, 5 week-old male immunocompromised mice (CB17-SCRF—Taconic, Hudson NY) were inoculated in the left cardiac ventricle with 5×10^4 PC3-ML cells stably expressing DsRED2 fluorescent protein (pDsRed2-N1 vector, Clontech Laboratories Inc., Palo Alto, CA). All experiments were performed in accordance with NIH guidelines for the humane use of animals. All protocols involving the use of animals were approved by the IACUC committee at Drexel University College of Medicine.

Acute dissociation of cells from metastatic tumors

Tumors were identified by fluorescence stereomicroscopy. Each tissue specimen was gently minced with a blade and mechanically dissociated. Cancer cells were collected by centrifugation and used for the imaging experiments within 2 h from collection of tumor tissues.

Immunocytochemistry

Cells were fixed with 4% formalin and permeabilized using 0.2% Triton X-100. Rabbit anti–cleaved caspase-3 antibody (Cell signaling, #96615 used at 1:100) or mouse anti-Human Ki-67 antibody (Transduction Labs BD, #610968 used at 1:50) were detected by Cy3-conjugated secondary antibodies (Jackson ImmunoResearch, West Grove, PA) used at 1:200.

Cell cycle analysis

Cells were trypsinized, and processed for cell cycle analysis using fluorescence-activated cell sorting (FACS) using GuavaEasycyte (Guava Technologies, Hayward, CA). The data were acquired and analyzed using the CytoSoft software (v.5.3, Guava Technologies).

ELISA measurement of histone acetylation

Global Histone-H3 acetylation was measured by an ELISA based approach using the EpiQuik™ assay kit according to the manufacturer's instructions for adherent cells (Epigentek, Brooklyn, NY, USA).

Data and statistical analysis

The Area Under the Curve was calculated using a specific function of the Graph Prism software (GraphPad, San Diego, CA). Values are presented as the mean ± standard error of the mean (SEM). Statistical significance was determined using a two-tailed, non-parametric students *t*-test and calculated using Prism software, version 3.02.

Acknowledgments This work was supported in part by the W. W. Smith Charitable Trust Foundation and NIH (grant GM067892 to A.F.). The authors wish to thank Dr. Olimpia Meucci for critically reading the manuscript, Whitney Jamieson and Mike Russell in Fatatis laboratory for cancer cell inoculation and members of Meucci laboratory for helpful discussion.

References

1. Fidler IJ (2003) The pathogenesis of cancer metastasis: the 'seed and soil' hypothesis revisited. Nat Rev Cancer 3:453–458
2. Bussard KM, Gay CV, Mastro AM (2008) The bone microenvironment in metastasis: what is special about bone? Cancer Metastasis Rev 27:41–55
3. Berridge MJ, Bootman MD, Roderick HL (2003) Calcium signalling: dynamics, homeostasis and remodelling. Nat Rev Mol Cell Biol 4:517–529
4. Orrenius S, Zhivotovsky B, Nicotera P (2003) Regulation of cell death: the calcium-apoptosis link. Nat Rev Mol Cell Biol 4:552–565
5. Mattson MP, Chan SL (2003) Calcium orchestrates apoptosis. Nat Cell Biol 5:1041–1043
6. Berger CE, Rathod H, Gillespie JI, Horrocks BR, Datta HK (2001) Scanning electrochemical microscopy at the surface of bone-resorbing osteoclasts: evidence for steady-state disposal and intracellular functional compartmentalization of calcium. J Bone Mineral Res 16:2092–2102
7. Skryma R et al (2000) Store depletion and store-operated Ca^{2+} current in human prostate cancer LNCaP cells: involvement in apoptosis. J Physiol 527.1:71–83
8. Prevarskaya N, Skryma R, Shuba Y (2004) Ca^{2+} homeostasis in apoptotic resistance of prostate cancer cells. Biochem Biophys Res Commun 322:1326–1335
9. Roderick HL, Cook SJ (2008) Ca^{2+} signalling checkpoints in cancer: remodelling Ca^{2+} for cancer cell proliferation and survival. Nat Rev Cancer 8:361–375
10. Russell MR, Jamieson WL, Dolloff NG, Fatatis A (2009) The alpha-receptor for platelet-derived growth factor as a target for antibody-mediated inhibition of skeletal metastases from prostate cancer cells. Oncogene 28:412–421
11. Chambers AF, Groom AC, Macdonald IC (2002) Dissemination and growth of cancer cells in metastatic sites. Nat Rev Cancer 8:563–572

12. Erb L, Liao Z, Seye CI, Weisman GA (2006) P2 receptors: intracellular signaling. Pflugers Arch 452:552–562
13. Vanoverberghe K, Mariot P, Vanden Abeele F, Delcourt P, Parys JB, Prevarskaya N (2003) Mechanisms of ATP-induced calcium signaling and growth arrest in human prostate cancer cells. Cell Calcium 34:75–85
14. Ichikawa J, Gemba H (2009) Cell density-dependent changes in intracellular Ca^{2+} mobilization via the P2Y(2) receptor in rat bone marrow stromal cells. J Physiol 219:372–381
15. Nemeth JA, Harb JF, Barroso U Jr, He Z, Grignon DJ, Cher ML (1999) Severe combined immunodeficient-hu model of human prostate cancer metastasis to human bone. Cancer Res 59:1987–1993
16. Mastro AM et al (2004) Breast cancer cells induce osteoblast apoptosis: a possible contributor to bone degradation. J Cell Biochem 91:265–267
17. Vantyghem SA et al (2005) A new model for lymphatic metastasis: development of a variant of the MDA-MB-468 human breast cancer cell line that aggressively metastasizes to lymph nodes. Clin Exp Metastasis 22:351–361
18. Van der Pluijm G et al (2005) Interference with the microenvironmental support impairs the de novo formation of bone metastases in vivo. Cancer Res 65:7682–7690
19. Buijs JT, van der Pluijm G (2009) Osteotropic cancers: from primary tumor to bone. Cancer Lett 273:177–193
20. Kratchmarova I, Blagoev B, Haack-Sorensen M, Kassem M, Mann M (2005) Mechanism of divergent growth factor effects in mesenchymal stem cell differentiation. Science 308:1472–1477
21. Sordi V, Malosio ML, Marchesi F, Mercalli A, Melzi R, Giordano T, Belmonte N, Ferrari G, Leone BE, Bertuzzi F, Zerbini G, Allavena P, Bonifacio E, Piemonti L (2005) Bone marrow mesenchymal stem cells express a restricted set of functionally active chemokine receptors capable of promoting migration to pancreatic islets. Blood 106:419–427
22. Bianco P, Riminucci M, Gronthos S, Gheron Robey P (2001) Bone marrow stromal stem cells: nature, biology, and potential applications. Stem Cells 19:180–192
23. Honczarenko M, Le Y, Swierkowski M, Ghiran I, Glodek A, Silberstein LE (2006) Human bone marrow stromal cells express a distinct set of biologically functional chemokine receptors. Stem Cells 24:1030–1041
24. Pinski J, Parikh A, Bova GS, Isaacs JT (2001) Therapeutic implications of enhanced G(0)/G(1) checkpoint control induced by coculture of prostate cancer cells with osteoblasts. Cancer Res 61:6372–6376
25. Bossy-Wetzel E, Green DR (1999) Caspases induce cytochrome c release from mitochondria by activating cytosolic factors. J Bio Chem 274:17484–17490
26. Scholzen T, Gerdes J (2000) The Ki-67 protein: from the known and the unknown. J Cell Physiol 182:311–322
27. Hu M, Polyak K (2008) Molecular characterisation of the tumour microenvironment in breast cancer. Eur J Cancer 44:2760–2765
28. Barkan D, Kleinman H, Simmons JL, Asmussen H, Kamaraju AK, Hoenorhoff MJ, Liu ZY, Costes SV, Cho EH, Lockett S, Khanna C, Chambers AF, Green JE (2008) Inhibition of metastatic outgrowth from single dormant tumor cells by targeting the cytoskeleton. Cancer Res 68:6241–6250
29. Goldberg AD, Allis CD, Bernstein E (2007) Epigenetics: a landscape takes shape. Cell 128:635–638
30. Bernstein BE, Meissner A, Lander ES (2007) The mammalian epigenome. Cell 128:669–681
31. Ateeq B, Unterberger A, Szyf M, Rabbani SA (2008) Pharmacological inhibition of DNA methylation induces proinvasive and prometastatic genes in vitro and in vivo. Neoplasia 10:266–278
32. Szyf M (2008) Epigenetics, DNA methylation, and chromatin modifying drugs. Annu Rev Pharmacol Toxicol 49:243–263
33. Bansal G, Druey KM, Xie Z (2007) R4 RGS proteins: regulation of G-protein signaling and beyond. Pharmacol Ther 116:473–495
34. Fatatis A, Caporaso R, Iannotti E, Bassi A, Di Renzo G, Annunziato L (1994) Relationship between time of activation of phospholipase C-linked plasma membrane receptors and reloading of intracellular Ca^{2+} stores in LAN-1 human neuroblastoma cells. J Biol Chem 269:18021–18027
35. Grimaldi M (2006) Astrocytes refill intracellular Ca2+ stores in the absence of cytoplasmic [Ca^{2+}] elevation: a functional rather than a structural ability. J Neurosci Res 84:1738–1749
36. Malli R, Frieden M, Hunkova M, Trenker M, Graier WF (2007) Ca^{2+} refilling of the endoplasmic reticulum is largely preserved albeit reduced Ca^{2+} entry in endothelial cells. Cell Calcium 41:63–76
37. Monteith GR, McAndrew D, Faddy HM, Roberts-Thomson SJ (2007) Calcium and cancer: targeting Ca^{2+} transport. Nat Rev Cancer 7:519–530
38. Darby PJ, Kwan CY, Daniel EE (1993) Use of calcium pump inhibitors in the study of calcium regulation in smooth muscle. Biol Signals 2:293–304
39. Lipskaia L, Hulot JS, Lompré AM (2009) Role of sarco/endoplasmic reticulum calcium content and calcium ATPase activity in the control of cell growth and proliferation. Pflugers Arch 457:673–685
40. Parekh AB, Penner R (1997) Store-operated calcium influx. Physiol Rev 77:901–930
41. Parekh AB, Putney JW (2005) Store-operated calcium channels. Physiol Rev 85:757–810
42. Dolloff NG, Russell MR, Loizos N, Fatatis A (2007) Human bone marrow activates the Akt pathway in metastatic prostate cells through transactivation of the alpha-platelet-derived growth factor receptor. Cancer Res 67:555–562
43. Hajnóczky G et al (2006) Mitochondrial calcium signalling and cell death: approaches for assessing the role of mitochondrial Ca^{2+} uptake in apoptosis. Cell calcium 40:553–560
44. Tombal B, Weeraratna AT, Denmeade SR, Isaacs JT (2000) Thapsigargin induces a calmodulin/calcineurin-dependent apoptotic cascade responsible for the death of prostatic cancer cells. Prostate 43:303–317
45. Yang GS, Zhang JJ, Huang XY (2009) Orai1 and STIM1 are critical for breast tumor cell migration and metastasis. Cancer Cell 15:124–134
46. Thebault HS, Flourakis M, Vanoverberghe K, Vandermoere K, Roudbaraki M, Lehen'kyi V, Slomianny C, Beck B, Mariot P, Bonnal JL, Mauroy B, Shuba Y, Capiod T, Skryma R, Prevarskaya N (2006) Differential role of transient receptor potential channels in Ca^{2+} entry and proliferation of prostate cancer epithelial cells. Cancer Res 66:2038–2047
47. Wang M, Stearns ME (1991) Isolation and characterization of PC-3 human-prostatic tumor sublines which preferentially metastasize to select organs in SCID mice. Differentiation 48:115–125
48. Meucci O, Fatatis A, Simen AA, Bushell TJ, Gray PW, Miller RJ (1998) Chemokines regulate hippocampal neuronal signaling and gp120 neurotoxicity. Proc Natl Acad Sci USA 95:14500–14505
49. Fatatis A, Miller RJ (1997) Platelet-derived growth factor (PDGF)-induced Ca^{2+} signaling in the CG4 oligodendroglial cell line and in transformed oligodendrocytes expressing the beta-PDGF receptor. J Biol Chem 272:4351–4358
50. Davis PK, Ho A, Dowdy SF (2001) Biological methods for cell-cycle synchronization of mammalian cells. Biotechniques 30:1322–1331